ABoVE: Tundra Plant Functional Type Continuous-Cover, North Slope, Alaska, 2010-2015

Get Data

Documentation Revision Date: 2021-08-27

Dataset Version: 1

Summary

This dataset provides predicted continuous-field cover for tundra plant functional types (PFTs), across ~125,000 km2 of Alaska's North Slope at 30 m resolution. The data cover the period 2010-07-01 to 2015-08-31. The data were derived using a random forest data-mining algorithm, predictors derived from Landsat satellite observations (surface reflectance composites for ~15-day periods from May-August), and field vegetation cover and site characterization data spanning bioclimatic and geomorphic gradients. The field vegetation cover was stratified by nine PFTs, plus open water, bare ground, and litter, and using the cover metrics total cover (areal cover including the understory) and top cover (uppermost canopy or ground cover), resulting in a total of 19 field cover types. The field data and predictor values at the field sites are also included.

Continuous-cover field maps have many advantages over traditional thematic maps, and the methods used here are well-suited to support periodic cover updates in tandem with future field and Landsat observations.

There are 39 data files included in this dataset. Continuous coverage data are provided in GeoTIFF (*.tif) format for 19 field cover types, each in two projections: Alaska Albers Equal Area Conic (EPSG:3338) and the ABoVE standard projection, Canada Albers Equal Area Conic (EPSG:102001) for a total of 38 files. The field data and predictors used in modeling are provided in one comma-separated file (*.csv).

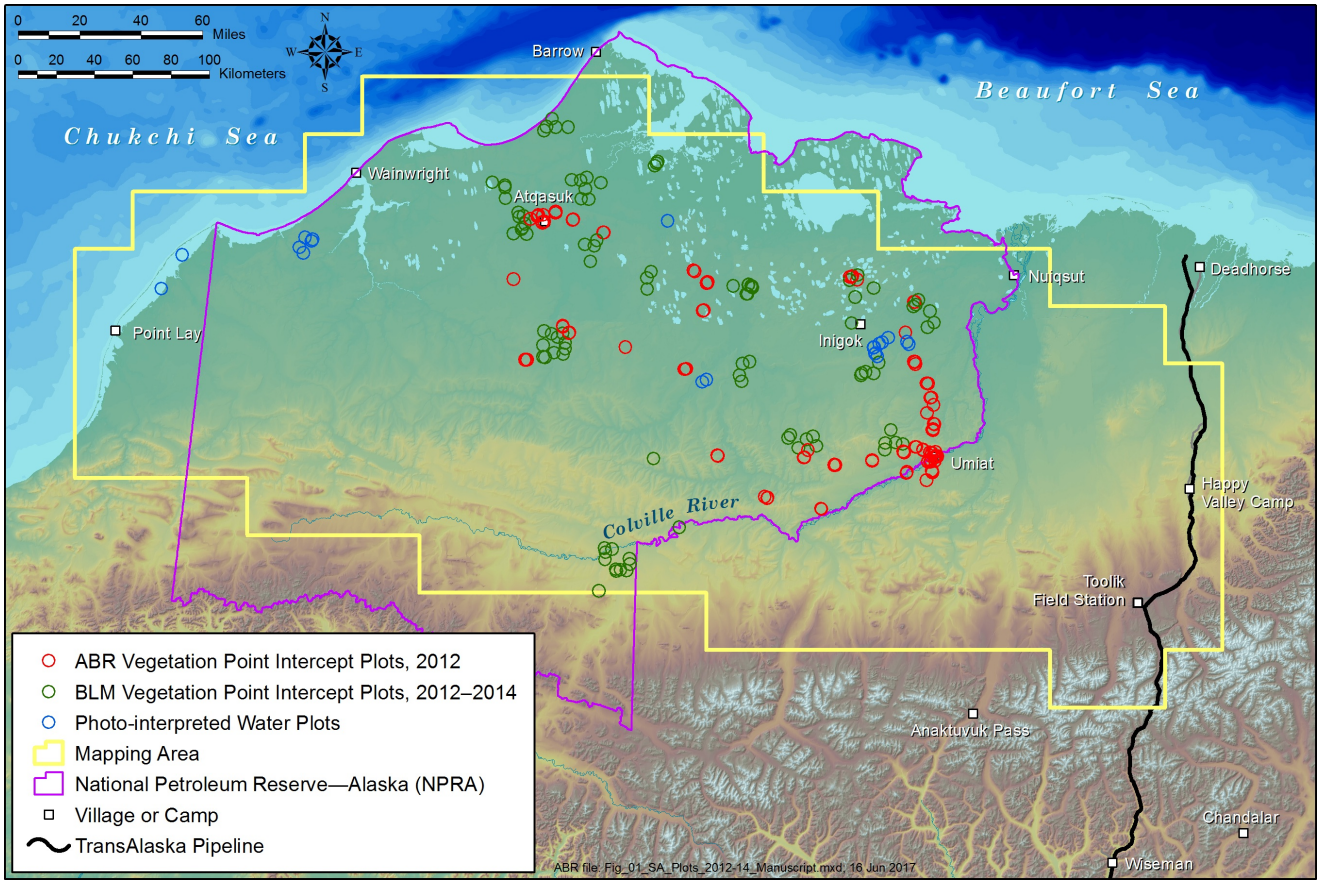

Figure 1. Map of quantitative-cover mapping area showing the distribution of field plots, North Slope, Alaska. ABR is ABR, Inc.-Environmental Research & Services and BLM is the Bureau of Land Management. Source: Macander et al., 2017

Citation

Macander, M.J., G.V. Frost, P.R. Nelson, and C.S. Swingley. 2020. ABoVE: Tundra Plant Functional Type Continuous-Cover, North Slope, Alaska, 2010-2015. ORNL DAAC, Oak Ridge, Tennessee, USA. https://doi.org/10.3334/ORNLDAAC/1830

Table of Contents

1. Dataset Overview

This dataset provides predicted continuous-field cover for tundra plant functional types (PFTs), across ~125,000 km^2 of Alaska's North Slope at 30 m resolution. The data cover the period 2010-07-01 to 2015-08-31. The data were derived using a random forest data-mining algorithm, predictors derived from Landsat satellite observations (surface reflectance composites for ~15-day periods from May-August), and field vegetation cover and site characterization data spanning bioclimatic and geomorphic gradients. The field vegetation cover was stratified by nine PFTs, plus open water, bare ground, and litter, and using the cover metrics total cover (areal cover including the understory) and top cover (uppermost canopy or ground cover), resulting in a total of 19 field cover types. The field data and predictor values at the field sites are also included.

Continuous-cover field maps have many advantages over traditional thematic maps, and the methods used here are well-suited to support periodic cover updates in tandem with future field and Landsat observations.

Project: Arctic-Boreal Vulnerability Experiment

The Arctic-Boreal Vulnerability Experiment (ABoVE) is a NASA Terrestrial Ecology Program field campaign based in Alaska and western Canada between 2016 and 2021. Research for ABoVE links field-based, process-level studies with geospatial data products derived from airborne and satellite sensors, providing a foundation for improving the analysis and modeling capabilities needed to understand and predict ecosystem responses and societal implications.

Related Publication

Macander, M., G. Frost, P. Nelson, and C. Swingley. 2017. Regional Quantitative Cover Mapping of Tundra Plant Functional Types in Arctic Alaska. Remote Sensing 9:1024. https://doi.org/10.3390/rs9101024

Related Datasets

For datasets related to vegetation in Alaska refer to additional ABoVE datasets.

Acknowledgments

This study was funded by the NASA ABoVE project (grant NNX17AE44G).

2. Data Characteristics

Spatial Coverage: Alaska's North Slope

> **ABoVE Reference Locations**
>
> Domain: Core ABoVE
>
> Grid cells (30 m): Bh006v000, Bh007v000, Bh006v001, Bh007v001, Bh008v001, Bh006v002, Bh007v002, Bh008v002, Bh007v003, Bh008v003

Spatial Resolution: 30 m

Temporal Coverage: 2010-05-16 to 2015-08-31

Temporal Resolution: One-time estimates

Study Area: Latitude and longitude are given in decimal degrees.

Sites	Westernmost Longitude	Easternmost Longitude	Northernmost Latitude	Southernmost Latitude
North Slope	-167.4761	-143.978	73.8004	65.5858

Data file information

There are 39 data files included in this dataset. Continuous coverage data are provided in GeoTIFF (*.tif) format for 19 field cover types, each in two projections: Alaska Albers Equal Area Conic (EPSG:3338) and the ABoVE standard projection, Canada Albers Equal Area Conic (EPSG:102001) for a total of 38 files. The field data and predictors used in modeling are provided in one comma-separated file (*.csv) Model_Training_Testing_Data.csv. The 133 variables are described in Table 2.

The GeoTIFF files are named according to the PFT and summarized measurements of the PFTs (Table 3) and cover metrics total cover (areal cover including the understory) and top cover (uppermost canopy or ground cover). The data are continuous-field percent ground cover for PFTs at 30 m resolution across ~125,000 km^2 of Alaska's North Slope.

Table 1. GeoTIFF File Names. The PFTs and other cover types are described in Table 3.

Files in Alaska Albers Equal Area Conic Projection (EPSG:3338)	Files in ABoVE Standard Projection (EPSG:102001)
Bare_Ground_Top_Cover.tif	Bare_Ground_Top_Cover_102001.tif
Bryophyte_Total_Cover.tif	Bryophyte_Total_Cover_102001.tif
Dwarf_Deciduous_Shrub_Total_Cover.tif	Dwarf_Deciduous_Shrub_Total_Cover_102001.tif
Dwarf_Evergreen_Shrub_Total_Cover.tif	Dwarf_Evergreen_Shrub_Total_Cover_102001.tif
Forb_Total_Cover.tif	Forb_Total_Cover_102001.tif
Grass_Total_Cover.tif	Grass_Total_Cover_102001.tif
Lichen_Total_Cover.tif	Lichen_Total_Cover_102001.tif

Litter_Top_Cover.tif	Litter_Top_Cover_102001.tif
Low_and_Tall_Deciduous_Shrub_Total_Cover.tif	Low_and_Tall_Deciduous_Shrub_Total_Cover_102001.tif
Low_Deciduous_Shrub_Total_Cover.tif	Low_Deciduous_Shrub_Total_Cover_102001.tif
Nonvascular_Plant_Top_Cover.tif	Nonvascular_Plant_Top_Cover_102001.tif
Nonvascular_Plant_Total_Cover.tif	Nonvascular_Plant_Total_Cover_102001.tif
Open_Water_Top_Cover.tif	Open_Water_Top_Cover_102001.tif
Sedge_Total_Cover.tif	Sedge_Total_Cover_102001.tif
Tall_Deciduous_Shrub_Total_Cover.tif	Tall_Deciduous_Shrub_Total_Cover_102001.tif
Total_Herbaceous_Total_Cover.tif	Total_Herbaceous_Total_Cover_102001.tif
Total_Shrub_Total_Cover.tif	Total_Shrub_Total_Cover_102001.tif
Vascular_Plant_Top_Cover.tif	Vascular_Plant_Top_Cover_102001.tif
Vascular_Plant_Total_Cover.tif	Vascular_Plant_Total_Cover_102001.tif

Data File Details

For all geoTIFF files:

- There are two projections; Alaska Albers Equal Area Conic (EPSG:3338) and the ABoVE standard projection, Canada Albers Equal Area Conic (EPSG:102001)
- The no data value is represented by "255"
- There is a single bands
- Map units are in meters

Table 2. Variables in the file Model_Training_Testing Data.csv. **User Note:** Many of the variables have a scale factor. All spectral indices are "Scaled by factor of 10000". Slope and snow free days have a scale factor of 100. Elevation is reported in decimeters.

Variable	Units	Description
plot_id		Unique name identifying the sample location
sample_date	YYYY-MM-DD	Date when field sampling occurred
line_length	m	Length of each sampling line
plot_radius	m	Radius of plot
source		Name of the field sampling campaign (ABR 2012, NPRA AIM, ABR Office) described in Section 5.
longitude	decimal degrees	Longitude in decimal degrees
latitude	decimal degrees	Latitude in decimal degrees
x_coord	m	X coordinate, EPSG 3338
y_coord	m	Y coordinate, EPSG 3338
train_test		Identifies whether data was in the training or reserved validation set
totalcover_shrubs	%	Total cover of shrubs
totalcover_d_low_tall_shrubs	%	Total cover of deciduous low and tall shrubs
totalcover_d_tall_shrubs	%	Total cover of deciduous tall shrubs
totalcover_d_low_shrubs	%	Total cover of deciduous low shrubs
totalcover_d_shrubs	%	Total cover of deciduous shrubs
totalcover_e_shrubs	%	Total cover of evergreen shrubs
totalcover_sedges_rush	%	Total cover of sedges and rushes
totalcover_grasses	%	Total cover of grasses
totalcover_forbs_ferns	%	Total cover of forbs and ferns
totalcover_vascular	%	Total cover of vascular plants
totalcover_nonvascular	%	Total cover of nonvascular plants
totalcover_mosses	%	Total cover of mosses
totalcover_lichens	%	Total cover of lichens
totalcover_liverworts	%	Total cover of liverworts
totalcover_algae	%	Total cover of algae
totalcover_dwarfshrub	%	Total cover of dwarf shrub
totalcover_herbs	%	Total cover of herbs (grasses, sedges, forbs)
totalcover_bryophytes	%	Total cover of bryophytes (liverworts and mosses)
topcover_shrubs	%	Top cover of shrubs

topcover_d_low_tall_shrubs	%	Top cover of deciduous low and tall shrubs
topcover_d_tall_shrubs	%	Top cover of deciduous tall shrubs
topcover_d_low_shrubs	%	Top cover of deciduous low shrubs
topcover_d_shrubs	%	Top cover of deciduous shrubs
topcover_e_shrubs	%	Top cover of evergreen shrubs
topcover_sedges_rush	%	Top cover of sedges and rushes
topcover_grasses	%	Top cover of grasses
topcover_forbs_ferns	%	Top cover of forbs and ferns
topcover_vascular	%	Top cover of vascular plants
topcover_nonvascular	%	Top cover of nonvascular plants
topcover_mosses	%	Top cover of mosses
topcover_lichens	%	Top cover of lichens
topcover_liverworts	%	Top cover of liverworts
topcover_algae	%	Top cover of algae
topcover_litter	%	Top cover of litter
topcover_water	%	Top cover of water
topcover_bareground	%	Top cover of bare ground
mean_woody_height	cm	Mean woody height by AIM method
woody_se	cm	Standard error of woody height by AIM method
count_woody_height		Count of height points where woody vegetation was present
mean_herb_height	cm	Mean herbaceous height by AIM method
herb_se	cm	Standard error of herbaceous height by AIM method
count_herb_height		Count of height points where herbaceous vegetation was present
count_heights_sampled		Count of height points
count_points_sampled		Count of vegetation point intercept points
vascular_species_richness		Vascular species richness
band1i_l_spr	Scaled by factor of 10000	Spring surface reflectance, Landsat 7 band 1
band2i_l_spr	Scaled by factor of 10000	Spring surface reflectance, Landsat 7 band 2
band3i_l_spr	Scaled by factor of 10000	Spring surface reflectance, Landsat 7 band 3
band4i_l_spr	Scaled by factor of 10000	Spring surface reflectance, Landsat 7 band 4
band5i_l_spr	Scaled by factor of 10000	Spring surface reflectance, Landsat 7 band 5
band7i_l_spr	Scaled by factor of 10000	Spring surface reflectance, Landsat 7 band 6
ndvi_l_spr	Scaled by factor of 10000	Spring Normalized Difference Vegetation Index (NDVI)
nbr_l_spr	Scaled by factor of 10000	Spring Normalized Burn Ratio (NBR)
ndmi_l_spr	Scaled by factor of 10000	Spring Normalized Difference Moisture Index (NDMI)
ndsi_l_spr	Scaled by factor of 10000	Spring Normalized Difference Snow Index (NDSI)
ndwi_l_spr	Scaled by factor of 10000	Spring Normalized Difference Water Index (NDWI)
evi2_l_spr	Scaled by factor of 10000	Spring Enhanced Vegetation Index (EVI)
band1i_l_0608	Scaled by factor of 10000	Early June surface reflectance, Landsat 7 band 1
band2i_l_0608	Scaled by factor of 10000	Early June surface reflectance, Landsat 7 band 2
band3i_l_0608	Scaled by factor of 10000	Early June surface reflectance, Landsat 7 band 3
band4i_l_0608	Scaled by factor of 10000	Early June surface reflectance, Landsat 7 band 4
band5i_l_0608	Scaled by factor of 10000	Early June surface reflectance, Landsat 7 band 5
band7i_l_0608	Scaled by factor of 10000	Early June surface reflectance, Landsat 7 band 6
ndvi_l_0608	Scaled by factor of 10000	Early June NDVI
nbr_l_0608	Scaled by factor of 10000	Early June NBR
ndmi_l_0608	Scaled by factor of 10000	Early June NDMI
ndsi_l_0608	Scaled by factor of 10000	Early June NDSI
ndwi_l_0608	Scaled by factor of 10000	Early June NDWI
evi2_l_0608	Scaled by factor of 10000	Early June EVI

band1i_l_0623	Scaled by factor of 10000	Late June surface reflectance, Landsat 7 band 1
band2i_l_0623	Scaled by factor of 10000	Late June surface reflectance, Landsat 7 band 2
band3i_l_0623	Scaled by factor of 10000	Late June surface reflectance, Landsat 7 band 3
band4i_l_0623	Scaled by factor of 10000	Late June surface reflectance, Landsat 7 band 4
band5i_l_0623	Scaled by factor of 10000	Late June surface reflectance, Landsat 7 band 5
band7i_l_0623	Scaled by factor of 10000	Late June surface reflectance, Landsat 7 band 6
ndvi_l_0623	Scaled by factor of 10000	Late June NDVI
nbr_l_0623	Scaled by factor of 10000	Late June NBR
ndmi_l_0623	Scaled by factor of 10000	Late June NDMI
ndsi_l_0623	Scaled by factor of 10000	Late June NDSI
ndwi_l_0623	Scaled by factor of 10000	Late June NDWI
evi2_l_0623	Scaled by factor of 10000	Late June EVI
band1i_l_0708	Scaled by factor of 10000	Early July surface reflectance, Landsat 7 band 1
band2i_l_0708	Scaled by factor of 10000	Early July surface reflectance, Landsat 7 band 2
band3i_l_0708	Scaled by factor of 10000	Early July surface reflectance, Landsat 7 band 3
band4i_l_0708	Scaled by factor of 10000	Early July surface reflectance, Landsat 7 band 4
band5i_l_0708	Scaled by factor of 10000	Early July surface reflectance, Landsat 7 band 5
band7i_l_0708	Scaled by factor of 10000	Early July surface reflectance, Landsat 7 band 6
ndvi_l_0708	Scaled by factor of 10000	Early July NDVI
nbr_l_0708	Scaled by factor of 10000	Early July NBR
ndmi_l_0708	Scaled by factor of 10000	Early July NDMI
ndsi_l_0708	Scaled by factor of 10000	Early July NDSI
ndwi_l_0708	Scaled by factor of 10000	Early July NDWI
evi2_l_0708	Scaled by factor of 10000	Early July EVI
band1i_l_0801	Scaled by factor of 10000	Midsummer surface reflectance, Landsat 7 band 1
band2i_l_0801	Scaled by factor of 10000	Midsummer surface reflectance, Landsat 7 band 2
band3i_l_0801	Scaled by factor of 10000	Midsummer surface reflectance, Landsat 7 band 3
band4i_l_0801	Scaled by factor of 10000	Midsummer surface reflectance, Landsat 7 band 4
band5i_l_0801	Scaled by factor of 10000	Midsummer surface reflectance, Landsat 7 band 5
band7i_l_0801	Scaled by factor of 10000	Midsummer surface reflectance, Landsat 7 band 6
ndvi_l_0801	Scaled by factor of 10000	Midsummer NDVI
nbr_l_0801	Scaled by factor of 10000	Midsummer NBR
ndmi_l_0801	Scaled by factor of 10000	Midsummer NDMI
ndsi_l_0801	Scaled by factor of 10000	Midsummer NDSI
ndwi_l_0801	Scaled by factor of 10000	Midsummer NDWI
evi2_l_0801	Scaled by factor of 10000	Midsummer EVI
band1i_l_0823	Scaled by factor of 10000	Late August surface reflectance, Landsat 7 band 1
band2i_l_0823	Scaled by factor of 10000	Late August surface reflectance, Landsat 7 band 2
band3i_l_0823	Scaled by factor of 10000	Late August surface reflectance, Landsat 7 band 3
band4i_l_0823	Scaled by factor of 10000	Late August surface reflectance, Landsat 7 band 4
band5i_l_0823	Scaled by factor of 10000	Late August surface reflectance, Landsat 7 band 5
band7i_l_0823	Scaled by factor of 10000	Late August surface reflectance, Landsat 7 band 6
ndvi_l_0823	Scaled by factor of 10000	Late August NDVI
nbr_l_0823	Scaled by factor of 10000	Late August NBR
ndmi_l_0823	Scaled by factor of 10000	Late August NDMI
ndsi_l_0823	Scaled by factor of 10000	Late August NDSI
ndwi_l_0823	Scaled by factor of 10000	Late August NDWI
evi2_l_0823	Scaled by factor of 10000	Late August EVI
slope_deg100	Degrees, scaled by factor of 100	Terrain slope

elevation	Decimeters	Elevation
summer_warmth_index100		Summer warmth index
snowfree_doy100	Day of year, scaled by factor of 100	Normal snow-free date
p_seas_water100	%	Water occurrence
ndvi_inc	Scaled by factor of 10000	NDVI amplitude (Midsummer NDVI minus Spring NDVI)

3. Application and Derivation

Ecosystem maps are foundational tools that support multi-disciplinary study design and applications including wildlife habitat assessment, monitoring, and earth-system modeling. Continuous-field maps have many advantages over traditional thematic maps. These methods are well-suited to support periodic map updates in tandem with future field and Landsat observations.

4. Quality Assessment

An assessment of model performance, including root mean squared error, mean absolute error and correlation for each cover type is provided in Macander et al. (2017; Table 4). This assessment was based on both internal cross-validation and iteratively reserving 20% of training data for validation. Selected shrub cover maps were compared to an existing fractional shrub cover map for the North Slope.

5. Data Acquisition, Materials, and Methods

Study area

The 125,000 km^2 mapping area extends from the Chukchi Sea near Point Lay eastward to the Dalton Highway (Fig. 1). The northern half of the mapping area is part of the Arctic Coastal Plain physiographic province (Gallant et al., 1995) characterized by flat topography, poorly drained soils, abundant water bodies, and widespread periglacial landforms such as ice-wedge polygons. Most of the Arctic Coastal Plain corresponds to Bioclimate Subzone D of the Circumpolar Arctic Vegetation Map (CAVM Team, 2003) shrubs are common, but they seldom exceed 1 m in height. The southern half of the mapping area encompasses the Arctic Foothills physiographic province and is characterized by widespread uplands dissected by well-defined drainage networks. The Arctic Foothills is situated in Bioclimate Subzone E, the warmest tundra subzone; shrubs are widespread, and tall thickets (>1.5 m height) are common on floodplains and adjacent slopes, particularly along the Colville River. Hereafter, the two major physiographic provinces are referred to as “coastal plain” and “foothills.” The entire mapping area lies in the zone of continuous permafrost.

Field Data

A field dataset of 106 plots in and near the National Petroleum Reserve-Alaska (NPRA) sampled during July–August 2012 (ABR, 2012) was pooled with 119 plots sampled by the BLM in 2012–2014 as part of the Bureau of Land Management's (BLM) Assessment, Inventory and Monitoring program (NPRA AIM). All field efforts utilized a point-intercept sampling method tailored for long-term monitoring of vegetation (Toevs et al., 2011); this protocol also facilitated sampling at scales appropriate for the analysis of 30 m resolution Landsat data. Plots sampled consisted of three 50 m lines; each line began 5 m from the plot center to avoid vegetation that was trampled during plot setup. The azimuth of the first line was selected randomly, and the others were offset from the first by 120 degrees. Vegetation “hits” were recorded at 1 m intervals using a rod-mounted laser pointer (51 sampling points per line), except at a few plots where logistical constraints necessitated quicker sampling at 2.5 m spacing (21 points per line). At each point, vegetation hits were identified by species by sequentially moving upper canopy leaves aside to allow the laser to hit underlying layers and finally the ground surface. For the ground surface, a single hit was recorded consisting either of live prostrate vegetation, litter, water, or bare ground. Although multiple hits were recorded in the field, only the first live hit for each species was retained for this analysis. The BLM data were collected using the same protocol except that lines were 25 m long and point spacing was 0.5 m (51 points per line).

BLM allocated plots according to a stratified random sampling design based on the 2013 North Slope Science Initiative (NSSI) Land Cover map (NSSI, 2013). Plot locations were subjectively selected in representative vegetation types based on photo signatures evident in 2.5 m resolution aerial imagery. Twenty water-only plots were identified from photo-interpreted satellite imagery within representative areas of clear and turbid water. Water-only plots comprised 9% of the total plot count, which matches the relative extent of open water portrayed on the NSSI map.

For analysis, the cover data were summarized by species, then aggregated to PFTs using two cover metrics: (1) total cover, the percent of sample points at which species belonging to a PFT occurred, summed for all species in a PFT; and (2) top cover, the percent of sample points at which a PFT was the first hit. Total cover values could exceed 100%, but top cover values could not exceed 100%. Importantly, because each species “hit” at a point was recorded and multiple species (including different species of the same PFT) could co-occur at different levels in the canopy, the sum of “total cover” values for all PFTs generally exceeded 100% and occasionally exceeded 100% for a single PFT; for example, in a very dense alder-willow shrubland with >50% cover of both species.

Table 3. Tundra PFTs and other cover types used for cover modeling, North Slope, Alaska (Macander et al., 2017).

PFT or Other Cover Type	Description	Cover Metric(s) Modeled
Tall Deciduous Shrubs	Deciduous shrubs ≥1.5 m height; mainly *Salix alaxensis, S. arbusculoides* and *Alnus fruticosa*	Total cover
Low Deciduous Shrubs	Deciduous shrubs 0.2–1.5 m height; e.g., *Betula nana, Salix pulchra*, and *S. glauca*	Total cover
Dwarf Deciduous Shrubs	Deciduous shrubs ≤0.2m height; e.g., *Salix rotundifolia, Arctous* spp., and *Vaccinium uliginosum*	Total cover
Dwarf Evergreen Shrubs	Evergreen shrubs ≤0.2m height; e.g., *Dryas integrifolia, Cassiope tetragona, Vaccinium vitis-ideas,* and *Ledum decumbens*	Total cover
Sedges	Herbaceous plants of *Cyperaceae* and *Juncaceae*; e.g., *Carex* and *Eriophorum* spp.	Total cover
Grasses	Herbaceous plants of *Poaceae*; e.g., *Arctagrostis, Arctophila, Deschampsia*	Total cover
Forbs	Non-graminoid herbaceous plants; e.g., legumes and composites	Total cover
Mosses	Total of all mosses and liverworts	Total cover
Lichens	Total of all ground lichens	Total cover

Total Herbaceous	Total of sedges, grasses, and forbs	Total cover
Total Shrubs	Total of all shrub PFTs	Total cover
Low and Tall Deciduous Shrubs	Deciduous shrubs ≥0.2 m in height	Total cover
Vascular Plants	Total of all vascular PFTs	Total and top cover
Nonvascular Plants	Total of all nonvascular PFTs including mosses, terricolous	Total and top cover
Litter	Dead plant matter	Top cover
Open Water	Open water	Top cover
Bare Ground	Bare soil or rock	Top cover

Spectral Predictors: Landsat Seasonal Composites

Calibrated, atmospherically corrected and precision terrain corrected (L1T) Landsat Surface Reflectance High-Level Data Products (Masek et al., 2007) derived from Landsat 4-5 Thematic Mapper (TM), Landsat 7 Enhanced Thematic Mapper (ETM+) and Landsat 8 Operational Land Imager (OLI) observations between 15 May and 31 August 1999–2015 were compiled. This date range captures the spring, summer, and early fall seasons on the North Slope.

Six seasonal Landsat composites were developed to represent ground conditions for key phenological windows from snowmelt to fall senescence using all available Landsat data for a specific date and year ranges. Each composite included six reflective bands as predictors (Table 4).

Table 4. Summary of spectral indices used for cover modeling, North Slope, Alaska.

Index	Formula	Reference
Normalized Difference Vegetation Index (NDVI)	(NIR − Red)/(NIR + Red)	Rouse et al., 1974; Tucker et al., 1979
Enhanced Vegetation Index-2 (EVI2)	(Red − Green)/(Red + [2.4 × Green] + 1)	Jiang et al., 2008
Normalized Difference Water Index (NDWI)	(Green − NIR)/(Green + NIR)	McFeeters et al., 1996
Normalized Difference Moisture Index (NDMI)	(NIR − SWIR1)/(NIR + SWIR1)	Goodwin et al., 2008
Normalized Difference Snow Index (NDSI)	(Green − SWIR1)/(Green + SWIR1)	Hall et al., 1995
Normalized Burn Ratio (NBR)	(NIR − SWIR2)/(NIR + SWIR2)	Key et al., 1999

To include more potential observations, a one-month seasonal window (16 July–15 August) was used to represent “midsummer”, the period of peak vegetation productivity. A longer year range (1999–2015) was used to construct the late August seasonal composite. The observation was selected with the median NIR reflectance value for each pixel for all seasonal windows except early June. Snow is usually widespread at that time, and both snow and green tundra have high NIR reflectance, so the observation was selected with the 20th percentile of NIR reflectance instead of the median.

Finally, a spring snow-free reflectance composite was developed to capture the temporally variable period after snowmelt, but before green-up by selecting the observation with the lowest NIR reflectance for each pixel. For NDVI, an “NDVI change” composite was produced representing the difference between midsummer and spring snow-free NDVI.

Regression models were trained with the randomForest algorithm (Breiman, 2001) using all predictors and the total cover was mapped for all PFTs, and the top cover for vascular plants, nonvascular plants, litter, water, and bare soil. Refer to Macander et al. (2017) for details.

6. Data Access

These data are available through the Oak Ridge National Laboratory (ORNL) Distributed Active Archive Center (DAAC).

ABoVE: Tundra Plant Functional Type Continuous-Cover, North Slope, Alaska, 2010-2015

Contact for Data Center Access Information:

- E-mail: uso@daac.ornl.gov
- Telephone: +1 (865) 241-3952

7. References

Breiman, L. 2001. Machine Learning 45:5–32. https://doi.org/10.1023/A:1010933404324

CAVM Team. 2003. Circumpolar Arctic Vegetation Map (1:7,500,000 Scale); Conservation of Arctic Flora and Fauna (CAFF) Map No. 1; U.S. Fish and Wildlife Service: Anchorage, AK, USA.

Gallant, A.L., E.F. Binnian, J.M. Omernik, and M.B. Shasby. 1995. Ecoregions of Alaska; U.S. Geological Survey Professional Paper 1567; United States Government Printing Office: Washington, DC, USA, p. 73.

Goodwin, N.R., N.C. Coops, M.A. Wulder, S. Gillanders, T.A. Schroeder, and T. Nelson. 2008. Estimation of insect infestation dynamics using a temporal sequence of Landsat data. Remote Sensing of Environment 112:3680–3689. https://doi.org/10.1016/j.rse.2008.05.005

Hall, D.K., G.A. Riggs, and V.V. Salomonson. 1995. Development of methods for mapping global snow cover using moderate resolution imaging spectroradiometer data. Remote Sensing of Environment 54:127–140. https://doi.org/10.1016/0034-4257(95)00137-P

Jiang, Z., A. Huete, K. Didan, and T. Miura. 2008. Development of a two-band enhanced vegetation index without a blue band. Remote Sensing of Environment 112:3833–3845. https://doi.org/10.1016/j.rse.2008.06.006

Key, C.H., and N.C. Benson. 1999. The Normalized Burn Ratio (NBR): A Landsat TM Radiometric Measure of Burn Severity; U.S. Geological Survey, Northern Rocky Mountain Science Center: Bozeman, MT, USA.

Macander, M., G. Frost, P. Nelson, and C. Swingley. 2017. Regional Quantitative Cover Mapping of Tundra Plant Functional Types in Arctic Alaska. Remote Sensing 9:1024. https://doi.org/10.3390/rs9101024

Masek, J.G., E.F. Vermote, N.E. Saleous, R. Wolfe, F.G. Hall, K.F. Huemmrich, F. Gao, J. Kutler, and T.-K. Lim. 2006. A Landsat Surface Reflectance Dataset for North America, 1990–2000. IEEE Geoscience and Remote Sensing Letters 3:68–72. https://doi.org/10.1109/LGRS.2005.857030

McFeeters, S.K. 1996. The use of the Normalized Difference Water Index (NDWI) in the delineation of open water features. International Journal of Remote Sensing 17:1425–1432. https://doi.org/10.1080/01431169608948714

North Slope Science Initiative (NSSI). 2013. North Slope Science Initiative Landcover Mapping Summary Report; Ducks Unlimited, Inc.: Rancho Cordova, CA, USA, p. 51.

Rouse, J.W., R.H. Haas, J.A Scheel, and D.W. Deering. 1974. Monitoring vegetation systems in the Great Plains with ERTS. In Proceedings of the 3rd Earth Resource Technology Satellite (ERTS) Symposium, Greenbelt, MD, USA, 10–14 December 1974; Volume 1, pp. 48–62.

Toevs, G.R., J.W. Karl, J.J. Taylor, C.S. Spurrier, M. “Sherm” Karl, M.R. Bobo, and J.E. Herrick. 2011. Consistent Indicators and Methods and a Scalable Sample Design to Meet Assessment, Inventory, and Monitoring Information Needs Across Scales. Rangelands 33:14–20. https://doi.org/10.2111/1551-501X-33.4.14

Tucker, C.J., J.H. Elgin, J.E. McMurtrey, and C.J. Fan. 1979. Monitoring corn and soybean crop development with hand-held radiometer spectral data. Remote Sensing of Environment 8:237–248. https://doi.org/10.1016/0034-4257(79)90004-X